

Multiple Bonds between Transition Metals and Main-Group Elements. 142.¹ Lewis-Base Adducts of Organorhenium(VII) Oxides: Structures and Dynamic Behavior in Solution

Wolfgang A. Herrmann,* Fritz E. Kühn,[†] Monika U. Rauch, João D. G. Correia, and Georg Artus

Anorganisch-chemisches Institut der Technischen Universität München, Lichtenbergstrasse 4, D-85747 Garching b. München, Germany

Received October 26, 1994[®]

Organorhenium(VII) oxides such as methyltrioxorhenium(VII) (**1**) and its longer-chain alkyl derivatives form 1:1 and 1:2 adducts with nitrogen-donor Lewis bases. These compounds adopt well-defined structures in the solid state. In solution, they undergo exchange of both the metal-coordinated base ligands and the oxo ligands. The synthesis and crystal structure (X-ray diffraction study) of the amino-functionalized complex

$\text{O}_3\text{Re}-\text{CH}_2\text{CH}_2\text{CH}_2\text{N}(\text{C}_5\text{H}_{10})$ (**3a**) is reported. Crystal data are as follows: monoclinic, space group $P2_1/c$, $a = 8.327(2)$ Å, $b = 11.516(1)$ Å, $c = 10.864(2)$ Å, $\beta = 101.54(7)^\circ$, $R = 0.028$ for 1747 reflections. Compounds of type **3a** are intramolecular base adducts in the solid state, but rigid geometries in solution can only be observed at low temperatures.

Introduction

There has been much recent interest in the nature, chemical behavior, and catalytic properties of transition metal oxo complexes.² Efficient syntheses of organorhenium(VII) oxides³ have entailed thorough reactivity and catalysis studies.⁴ Some of these compounds, e.g. methyltrioxorhenium(VII) and cyclopropyltrioxorhenium(VII),^{3f,5} are efficient catalysts in olefin oxidation,⁶ olefin metathesis,⁷ aldehyde olefination,⁸ Baeyer–

Villiger oxidation,⁹ arene oxidation,¹⁰ and metal carbonyl oxidation.¹¹ Electron-poor organorhenium(VII) oxides show a pronounced Lewis acidity at their metal centers, thus forming adducts with electron-donor ligands such as nitrogen bases.^{3hi,12} These adducts are also active in some of the above-mentioned catalytic processes. It is also true, however, that organorhenium(VII) oxides show reduced activity with higher selectivity in olefin epoxidation when amines or pyridines are present.⁵ Recently we reported on the influence of the ligand R on the ¹⁷O NMR spectra of R–ReO₃ compounds.^{13a} Since many derivatives of type R–ReO₃ are sufficiently stable only in the presence of nitrogen bases, there was a need to explore some structural phenomena regarding compounds of general formula R–ReO₃ⁿL with respect to their catalytic properties mentioned above.

Results and Discussion

(A) Organorhenium(VII) Oxides in Solution. (1) Solvent and Temperature Effects. As recently shown by NMR studies,¹³ the proton (α -¹H) and oxygen (¹⁷O) nuclei of organorhenium(VII) oxides, e.g. CH₃ReO₃ (**1**), exhibit strongly solvent-dependent chemical shifts. These effects are in good correlation with the Gutmann donor numbers.^{13b} Equilibria such

[†] Hermann Schlosser Foundation Fellow, 1992–1994.

[®] Abstract published in *Advance ACS Abstracts*, May 1, 1995.

- (1) Preceding paper of this series: Herrmann, W. A.; Roesky, P. W.; Elison, M.; Artus, G.; Öfele, K. *Organometallics* **1995**, *14*, 1085–1086.
- (2) Monographs and reviews: (a) Mayer, J. M.; Nugent, W. A. *Metal-Ligand Multiple Bonds*; Wiley: New York, 1988. (b) Sheldon, R. A.; Kochi, J. K. *Metal-Catalyzed Oxidations of Organic Compounds*; Academic Press: New York, 1981. (c) Jørgensen, K. A. *Chem. Rev.* **1989**, *89*, 431–458.
- (3) (a) Herrmann, W. A.; Serrano, R.; Bock, H. *Angew. Chem.* **1984**, *96*, 364–365; *Angew. Chem., Int. Ed. Engl.* **1984**, *23*, 383–385. (b) Herrmann, W. A.; Kuchler, J. G.; Felixberger, J. K.; Herdtweck, E.; Wagner, W. *Angew. Chem.* **1988**, *100*, 420–422; *Angew. Chem., Int. Ed. Engl.* **1988**, *27*, 394–396. (c) Herrmann, W. A.; Ladwig, M.; Kiprof, P.; Riede, J. *J. Organomet. Chem.* **1989**, *371*, C13–C15. (d) Herrmann, W. A.; Kühn, F. E.; Fischer, R. W.; Thiel, W. R.; Romão, C. C. *Inorg. Chem.* **1992**, *31*, 4431–4432. (e) Herrmann, W. A.; Romão, C. C.; Fischer, R. W.; Kiprof, P.; de Méric de Bellefon, C. *Angew. Chem.* **1991**, *103*, 183–185; *Angew. Chem., Int. Ed. Engl.* **1991**, *30*, 185–187. (f) Herrmann, W. A.; Kühn, F. E.; Romão, C. C.; Huy, Y. T.; Wang, M.; Fischer, R. W.; Kiprof, P.; Scherer, W. *Chem. Ber.* **1993**, *126*, 45–50. (g) Kühn, F. E.; Herrmann, W. A.; Hahn, R.; Elison, M.; Blümel, J.; Herdtweck, E. *Organometallics* **1994**, *13*, 1601–1607. (h) Herrmann, W. A.; Kühn, F. E.; Romão, C. C.; Tran Huy, H. *J. Organomet. Chem.*, in press. (i) de Méric de Bellefon, C.; Herrmann, W. A.; Kiprof, P.; Whitaker, C. R. *Organometallics* **1992**, *11*, 1072–1080.
- (4) Reviews: (a) Herrmann, W. A. *Angew. Chem.* **1988**, *100*, 1269–1286; *Angew. Chem., Int. Ed. Engl.* **1988**, *27*, 1297–1313. (b) Herrmann, W. A. *J. Organomet. Chem.* **1990**, *382*, 1–18.
- (5) Herrmann, W. A.; Fischer, R. W.; Rauch, M. U.; Scherer, W. *J. Mol. Catal.* **1994**, *86*, 243–266.
- (6) (a) Herrmann, W. A.; Fischer, R. W.; Marz, D. W. *Angew. Chem.* **1991**, *103*, 1706–1709; *Angew. Chem., Int. Ed. Engl.* **1991**, *30*, 1638–1641. (b) Herrmann, W. A.; Fischer, R. W.; Scherer, W.; Rauch, M. U. *Angew. Chem.* **1993**, *105*, 1209–1212; *Angew. Chem., Int. Ed. Engl.* **1993**, *32*, 1157–1160.
- (7) Herrmann, W. A.; Wagner, W.; Flessner, U. N.; Volkhardt, U.; Komber, H. *Angew. Chem.* **1991**, *103*, 1704–1706; *Angew. Chem., Int. Ed. Engl.* **1991**, *30*, 1636–1638.

- (8) (a) Herrmann, W. A.; Wang, M. *Angew. Chem.* **1991**, *103*, 1709–1711; *Angew. Chem., Int. Ed. Engl.* **1991**, *30*, 1641–1643. (b) Herrmann, W. A.; Roesky, P. W.; Wang, M.; Scherer, W. *Organometallics*, in press.
- (9) Herrmann, W. A.; Fischer, R. W.; Correia, J. D. G. *J. Mol. Catal.* **1994**, *94*, 213–223.
- (10) Adam, W.; Herrmann, W. A.; Lin, J.; Saha-Möller, C. R.; Fischer, R. W.; Correia, J. D. G. *Angew. Chem.* **1994**, *106*, 2545–2546; *Angew. Chem., Int. Ed. Engl.* **1994**, *33*, 2475–2476.
- (11) (a) Thiel, W. R.; Fischer, R. W.; Herrmann, W. A. *J. Organomet. Chem.* **1993**, *459*, C9–C11. (b) Herrmann, W. A.; Correia, J. D. G.; Kühn, F. E.; Artus, G. R. *J. Chemistry*, submitted for publication.
- (12) (a) Herrmann, W. A.; Kuchler, J. G.; Weichselbaumer, G.; Herdtweck, E.; Kiprof, P. *J. Organomet. Chem.* **1989**, *372*, 351–370. (b) Herrmann, W. A.; Weichselbaumer, G.; Herdtweck, E. *J. Organomet. Chem.* **1989**, *372*, 371–389. (c) Herrmann, W. A.; Kühn, F. E.; Romão, C. C.; Kleine, M.; Mink, J. *Chem. Ber.* **1994**, *127*, 47–54. (d) Herrmann, W. A.; Roesky, P. W.; Alberto, R.; Artus, G.; Scherer, W. *Inorg. Chem.*, submitted for publication.
- (13) (a) Herrmann, W. A.; Kühn, F. E.; Roesky, P. W. *J. Organomet. Chem.* **1995**, *485*, 243–251. (b) Kühn, F. E. Ph.D. Thesis, Technische Universität München, 1994.
- (14) Kuchler, J. G. Ph.D. Thesis, Technische Universität München, 1990.

Scheme 1

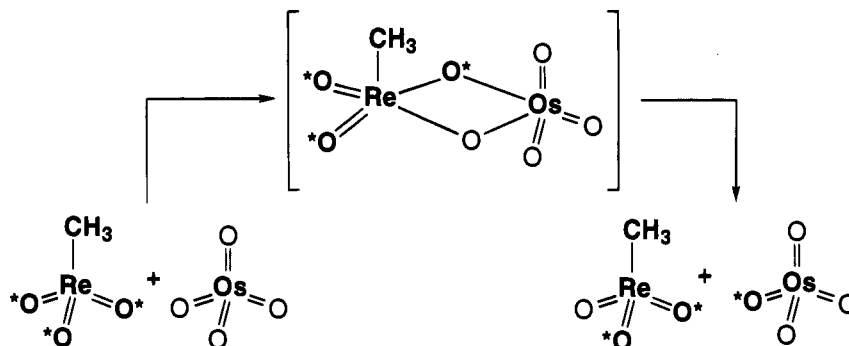
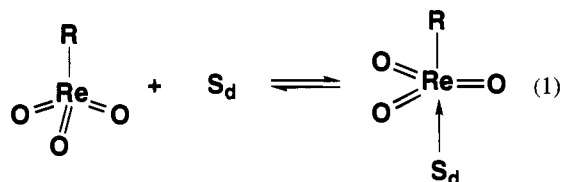


Table 1. Temperature-Dependent ^{17}O NMR Shifts for **1** in Various Solvents

temp ($^{\circ}\text{C}$)	thf		CDCl_3	
	$\delta(^{17}\text{O})$ (ppm)	$\Delta\nu_{1/2}$ (Hz)	$\delta(^{17}\text{O})$ (ppm)	$\Delta\nu_{1/2}$ (Hz)
50	857	130	823	80
20	872	130	822	130
-30	878	190	820	150
-60	881	290	819	170

as that of eq 1 explain this phenomenon.¹³ The ^{17}O NMR shifts of CH_3ReO_3 and its higher congeners RCH_2ReO_3 show a weak temperature effect only in polar solvents, e.g. thf, whereas in more or less "inert" solvents such as CHCl_3 and toluene no such effects occur (Table 1). The half-width of the ^{17}O NMR signal of **1** increases slightly with decreasing temperature (Table



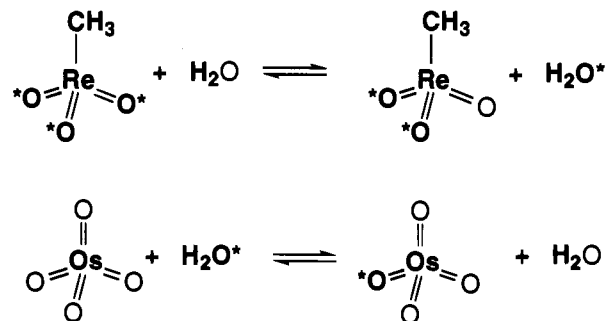
$\text{S}_d = \text{thf, RCN, ROH, pyridine, H}_2\text{O}$

1). At $-60\text{ }^{\circ}\text{C}$ the half-width is more than 2 times larger than that at $+50\text{ }^{\circ}\text{C}$. Such effects in ^{17}O NMR spectroscopy are known to result from increasing viscosity of the solvents at low temperatures.

(2) **Oxygen Exchange.** Stirring ^{17}O -labeled $\text{CH}_3\text{Re}(*\text{O})_3$ in the presence of OsO_4 in thf rapidly yields labeled $\text{Os}(*\text{O})_4$ ($\delta(^{17}\text{O}) = 806$ ppm). Both the signals of **1** and OsO_4 are temperature-independent. The chemical shifts are identical with those of authentic, pure compounds. This result shows that an oxygen exchange takes place if free coordination sites are available. It remains unclear whether traces of water¹⁵ or intermolecular oxygen bridges are responsible for the labeling effect. Even at low temperatures ($-80\text{ }^{\circ}\text{C}$ in thf) oxygen bridges are not observed in the ^{17}O NMR spectra. A water signal is not observed either, but (catalytic) traces of water could be sufficient to promote the oxygen exchange. Mechanisms of both Schemes 1 and 2 are thus possible.

CH_3ReO_3 exchanges its oxo ligands also with other coordinatively unsaturated organorhenium(VII) oxides, e.g. $\text{C}_2\text{H}_5\text{ReO}_3$ (**2**) and $(\text{H}_2\text{C}=\text{CHCH}_2)\text{ReO}_3$. The chemical shift of the compounds and the half-widths of the peaks are not influenced

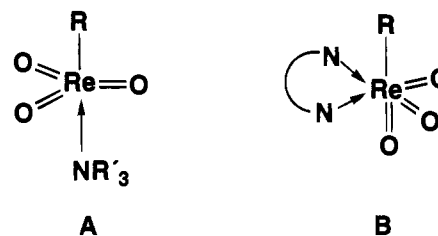
Scheme 2



by the presence of a second organorhenium(VII) oxide in solution and the oxygen exchange process.

By way of contrast no oxo ligand exchange is observed with the coordinatively saturated (η^5 -pentamethylcyclopentadienyl)trioxorhenium(VII) ($\delta(^{17}\text{O}) = 647$ ppm, CDCl_3), neither with ^{17}O -labeled water nor with ^{17}O -labeled **1**. (η^5 -Cyclopentadienyl)trioxorhenium(VII) ($\delta(^{17}\text{O}) = 691$ ppm, CDCl_3) shows a slow oxo exchange with ^{17}O -labeled **1**. We assume, that a hapticity shift $\eta^5 \rightleftharpoons \eta^3$ enables this reaction to occur.

(B) **Base Adducts of Organorhenium(VII) Oxides in Solution.** (1) **Solvent Effects.** Organorhenium(VII) oxides form two different types of base adducts: monodentate (A) and bidentate (B). In the present paper, typical examples of both



groups are described in terms of their behavior in solution. Monodentate base adducts show in most cases an even stronger low-field shift in the ^{17}O NMR spectra than the free organorhenium(VII) oxides $\text{R}-\text{ReO}_3$ in donor solvents like thf.¹³ This observation is in accord with the more pronounced σ -donor character of nitrogen as compared to oxygen donors. The strongest ^1H NMR upfield shifts are observed when the complexes $\text{R}-\text{ReO}_3$ are dissolved in liquid N-donor ligands such as pyridine or aniline. The chemical shift of CH_3ReO_3 (aniline) (**1a**) does not depend very much on the solvent ($\delta(^{17}\text{O})$: 849 ppm, toluene; 847 ppm, CDCl_3 ; 846 ppm, aniline), in contrast to an earlier statement.^{12b} This is not surprising since adducts of **1** (and other organorhenium oxides) with bulky bases have no space available for a donor solvent to enter the molecule.

(2) **Temperature Effects.** The ^{17}O NMR spectra show only one signal for 1/1 adducts of **1** (type A), even at low

(15) It is known that both OsO_4 and CH_3ReO_3 (cf. ref 13) exchange their oxo ligands with water: (a) Eder, S. J. Ph.D. Thesis, Technische Universität München, 1992. (b) For ^{17}O NMR spectral data of OsO_4 and related compounds, see: Edwards, C. F.; Griffith, W. P.; Williams, D. J. *J. Chem. Soc., Chem. Commun.* **1990**, 1523-1524.

(16) Herrmann, W. A.; Kleine, M.; Kühn, F. E.; Fischer, R. W. Unpublished results, 1991-1994.

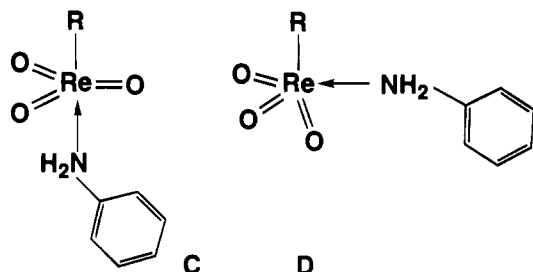
Table 2. Temperature-Dependent ^{17}O and ^1H NMR Data for **1** and **1a** in Toluene

temp ($^{\circ}\text{C}$)	1 $\delta(^{17}\text{O})$ (ppm)	1a $\delta(^{17}\text{O})$ (ppm)	1a $\delta(^1\text{H})(\text{NH}_2)$ (ppm)
		824 ^b	2.77
+80	825 ^a	846	2.76
+20	823	849	2.64
-20	821	860	2.52
-60	819	877	2.37

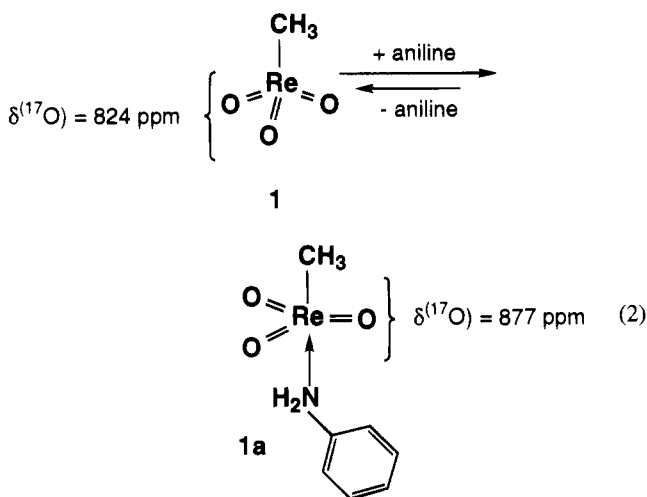
^a Pure starting materials: CH_3ReO_3 in toluene and aniline in toluene.

^b $\delta(^{17}\text{O})$ of CH_3ReO_3 in aniline at 0°C : 846 ppm ($\Delta\nu_{1/2} = 930$ Hz).

temperatures. The base ligand is located *trans* to the methyl group. The aniline adduct^{12b} **1a** exhibits one oxygen signal in the temperature range -60 to $+80^{\circ}\text{C}$. This is surprising because the two isomers **C** and **D** are seen in the solid state.



Upon cooling of **1a** from $+80$ to -60°C , the chemical shifts of the amine protons and of the oxygen atoms change significantly (Table 2). At room temperature and above, the ^1H NMR shift of the NH_2 protons is very similar to that for free aniline, and the ^{17}O NMR shift of the oxygen atoms resembles that of the oxygens in free CH_3ReO_3 (**1**); cf. Table 2. At lower temperatures the oxygen signals are much more low-field-shifted, while the NH_2 proton signals are significantly shifted to higher fields. These effects can only be rationalized in terms of the equilibrium of eq 2. Aniline is a weak Lewis



base forming only a labile adduct with the Lewis acid **1**. Higher temperatures suffice for quick (dissociative) exchange processes to occur. This equilibrium is frozen at low temperature, so only the *mer*-configuration is seen. In the case of pure CH_3ReO_3 , a similar equilibrium between uncoordinated and thf-coordinated **1** exists.

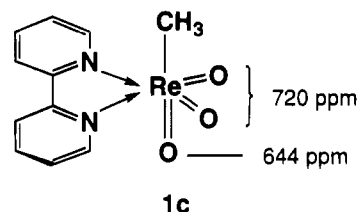
Heating or cooling a solution of $\text{CH}_3\text{ReO}_3(\text{quin})$ (**1b**) in CDCl_3 has no influence on the ^{17}O chemical shift ($\delta(^{17}\text{O}) = 907$ ppm, -60 to $+50^{\circ}\text{C}$). The obvious reason for this different behavior is the stronger Lewis basicity of quinuclidine ($pK_b =$

Table 3. Temperature-Dependent ^{17}O NMR Data for **1/1b**

cpd (ratio)	$\delta(^{17}\text{O})$ (ppm)	$\Delta\nu_{1/2}$ (Hz)	temp ($^{\circ}\text{C}$)
(a) In thf			
1b/1 (1:1)	893	250	40
1b/1 (1:1)	896	620	25
1b/1 (1:1)	894	850	12
1b/1 (1:1)	920	1300	0
	879	820	
1b/1 (1:1)	926	500	-15
	877	350	
1b/1 (1:1)	926	305	-30
	878	170	
(b) In CDCl_3			
1/1b (1:1)	860	800	50
1/1b (1:1)	907	1300	20
	822	840	
1/1b (1:1)	906	380	-30
	820	130	

3.45^{12b}), which ligand therefore coordinates more strongly to the Re center than the *much* weaker Lewis base aniline ($pK_b = 9.37^{12b}$).

The adduct **1c** of 4,4'-di-*tert*-butyl-2,2'-bipyridine with CH_3ReO_3 has an octahedral geometry in the solid state,^{12d} but the two expected ^{17}O peaks occur only at -30°C in the NMR

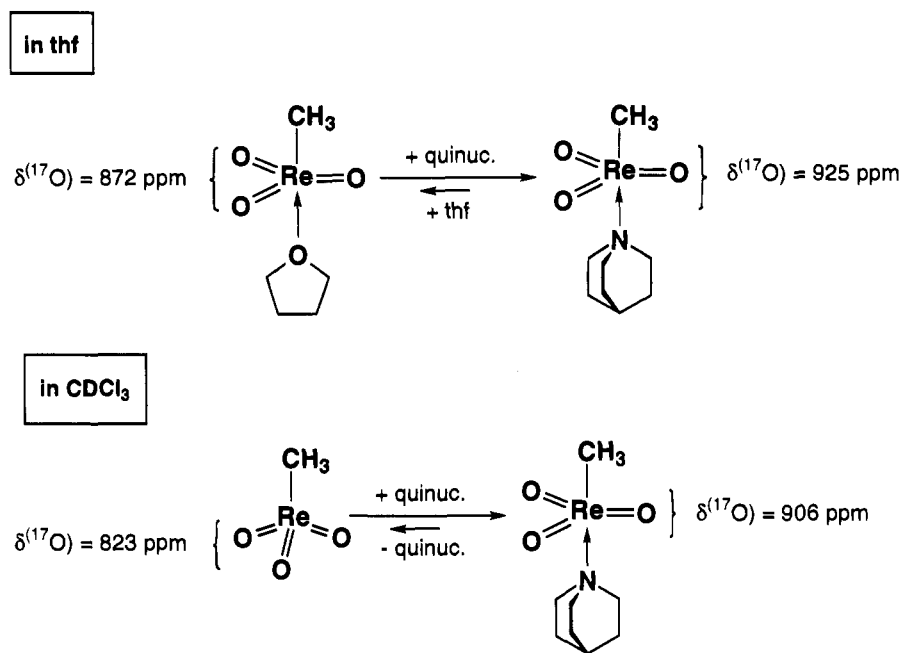


spectra. At room temperature a broad resonance is present,¹³ indicating rapid structural equilibration. To explore the nature of this exchange (pseudorotation or opening of the ligand), ^{17}O -labeling experiments were performed; cf. Section B.4.

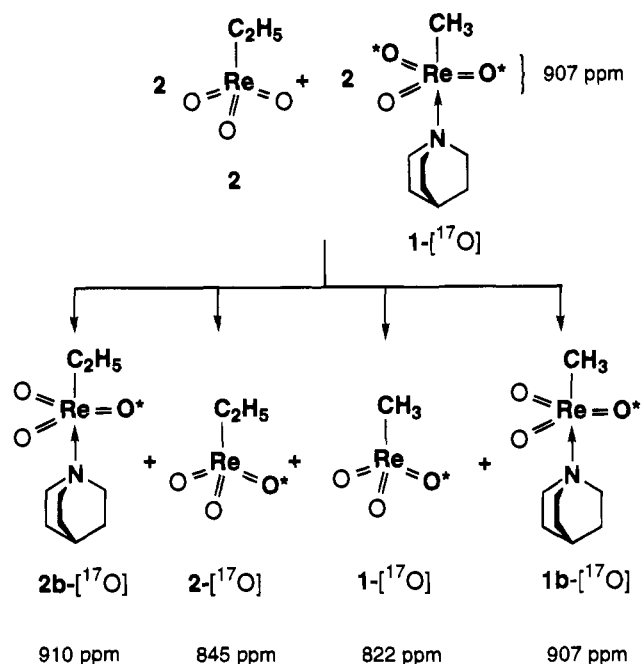
(3) Oxygen and Lewis Base Exchange Phenomena. The parent compound **1** is easily labeled by just adding H_2^{17}O to thf solutions.¹³ Labeled base adducts of **1** were prepared by reacting the isolated, sublimed $1\text{-}[^{17}\text{O}]$ with the respective N-ligands in diethyl ether (Experimental Section).

If $1b\text{-}[^{17}\text{O}]$ is treated in thf with unlabeled **1**, only *one peak* appears in the ^{17}O NMR spectra at 25°C . This peak represents neither **1** ($\delta(^{17}\text{O}) = 872$ ppm) nor **1b** ($\delta(^{17}\text{O}) = 925$ ppm). When equal amounts of **1** and **1b** are used, the signal occurs at $\delta \approx 896$ ppm (25°C); it is much broader than the signals of the authentic compounds (**1**: $\nu_{1/2} = 130$ Hz; **1b**, $\nu_{1/2} = 170$ Hz). Upon an increase in the temperature, a sharpening of the signal is seen, while cooling leads to a broader signal which begins to split up at *ca.* 0°C (Table 3a). Two well-separated signals with nearly the same ^{17}O NMR shift as the pure compounds **1** and **1b** are seen at -30°C . This phenomenon clearly results from a quick exchange of the base between labeled and unlabeled **1** at and above room temperature. The two different signals representing the starting materials (now both marked) are seen at low temperature. When an excess of **1b** is used, the signal at room temperature is closer to 925 ppm, and with an excess of **1**, it is closer to 872 ppm. When CDCl_3 is used as a solvent instead of thf, two signals occur even at room temperature (Table 3b). The obvious explanation is that CDCl_3 is not a donor solvent like thf, so no competition can occur between the strong Lewis base quinuclidine and the (excess) donor solvent. A dissociation equilibrium takes place at lower temperatures in donor solvents as compared to nondonating solvents (Scheme 3).

Scheme 3



Scheme 4



Proton NMR experiments support this explanation. When quinuclidine ($\delta(^1\text{H}) = 2.76$ (m) ($\text{N}(\text{CH}_2)_3$), 1.47 (m) ($\text{N}(\text{CH}_2\text{CH}_2)_2$), 1.63 (CH)) is added to the quinuclidine adduct of **1** ($\delta(^1\text{H}) = 2.47$ (m) ($\text{N}(\text{CH}_2)_3$), 1.52 (m) ($\text{N}(\text{CH}_2\text{CH}_2)_2$), 1.75 (m) (CH), 1.21 (s) (Re-CH₃)) in thf, only four signals can be observed at room temperature ($\delta(^1\text{H}) = 2.53$ (s, broad) ($\text{N}(\text{CH}_2)_3$), 1.50 (m) ($\text{N}(\text{CH}_2\text{CH}_2)_2$), 1.69 (m) (CH), 1.20 (s) (Re-CH₃)). This is again a clear indication for quick ligand exchange.

When ¹⁷O-labeled base adducts such as **1b** are mixed with a different unlabeled R-ReO₃ compound such as ethyltrioxorhenium(VII) (**2**) both base and oxo exchange can be observed in CHCl₃ (Scheme 4). If only base exchange took place, two signals should be observed after some time: **1**, $\delta(^{17}\text{O}) = 825$ ppm; **1b**, $\delta(^{17}\text{O}) = 907$ ppm (2000 scans; unlabeled compounds not seen under these conditions in the ¹⁷O NMR spectra). **2**

also forms readily a complex with quinuclidine^{3e} and should therefore abstract a certain fraction of quinuclidine from **1b**, and free CH₃ReO₃ (**1**) ($\delta(^{17}\text{O}) \approx 822$ ppm, $\Delta\nu_{1/2} = 130$ Hz) should remain from this reaction. If only oxygen exchange takes place, two signals should be observed, too: **1b** and **2** ($\delta(^{17}\text{O}) = 845$ ppm, $\Delta\nu_{1/2} = 130$ Hz). However, three signals are observed: one for CH₃Re(*O)₃ ($\delta(^{17}\text{O}) = 832$ ppm, $\Delta\nu_{1/2} = 170$ Hz), one for C₂H₅Re(*O)₃ ($\delta(^{17}\text{O}) = 845$ ppm, $\Delta\nu_{1/2} = 210$ Hz), and a very broad one ($\Delta\nu_{1/2} = 640$ Hz) for the quinuclidine adducts of CH₃Re(*O)₃ and C₂H₅Re(*O)₃ ($\delta(^{17}\text{O}) \approx 910$ ppm). The signals of the two latter compounds are so close that even at low temperatures (-30 °C) there is no splitting into two different signals.

A mixture of **1** and **1c** also shows exchange of the N-ligand. At room temperature and above, only one signal is observed, while three signals of **1** and **1c** occur at lower temperatures. This result shows that even bidentate base ligands undergo exchange reactions. The pronounced water sensitivity of bidentate base adducts is now easily explained: when the ligand opens free coordination sites via dissociation, OH⁻ (basic medium!) can coordinate to **1**. This leads to quick decomposition with formation of methane and perhenate.¹⁴ Base ligand adducts of **1** do not allow ¹⁷O enrichment by simple treatment with an excess of H₂¹⁷O because they decompose for the given reason (formation of perhenate, $\nu(\text{ReO}) \approx 909$ cm⁻¹, IR; $\delta(^{17}\text{O}) \approx 565$ ppm, NMR). If bidentate ligands would not dissociate from the metal, no such decomposition should occur.

The same experiment was repeated for labeled **1c** and unlabeled **2** in CHCl₃. Even with the bidentate ligand 4,4'-di-*tert*-butyl-2,2'-bipyridine, both N-ligand and oxo exchange takes place within ca. 15 min. The signals of **1**, **1c**, **2** and (4,4'-di-*tert*-butyl-2,2'-bipyridine)ethyltrioxorhenium (**2c**), $\delta(^{17}\text{O}) = 719$ and 627 ppm, were observed. The signals of **1c** and **2c** were so close together that they could not be distinguished. A significant broadening of the α -protons of **1**, **1c**, **2**, and **2c** was observed in the ¹H NMR spectra upon warming the solutions from -30 to $+20$ °C. This is also indicative of exchange processes.

(C) **Base-Functionalized Organorhenium(VII) Oxides.** (1) **Solid State Structure.** N-Functionalized alkylrhenium(VII) oxides form intramolecular base adducts.^{6b} The solid state

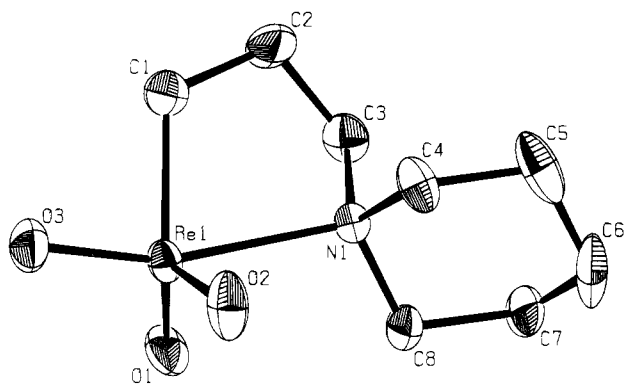


Figure 1. PLATON representation²² of the crystal and molecular structure of [3-(*N*-piperidyl)-*n*-propyl]trioxorhenium(VII) (**3a**). Thermal ellipsoids are at a 50% probability level. Hydrogen atoms are omitted for clarity.

Table 4. Selected Bond Distances (Å) and Angles (deg) of the (γ -Aminoalkyl)rhenium(VII) Oxide **3a** (Single-Crystal X-ray Diffraction)

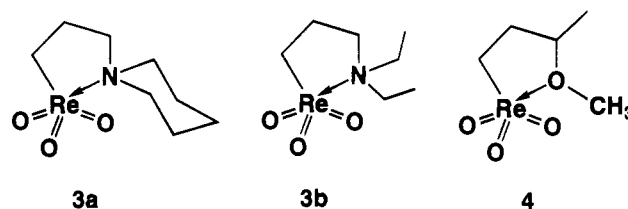
Re1–O1	1.706(4)	Re1–C1	2.123(6)
Re2–O2	1.695(4)	C1–C2	1.501(8)
Re3–O3	1.715(4)	C2–C3	1.512(9)
Re1–N1	2.385(4)	N1–C3	1.466(6)
O2–Re1–O1	116.5(2)	C3–N1–Re1	105.7(3)
O3–Re1–O1	106.5(2)	C4–N1–Re1	110.6(3)
O3–Re1–O2	104.6(2)	C4–N1–C3	112.1(4)
N1–Re1–O1	84.5(2)	C8–N1–Re1	108.8(3)
N1–Re1–O2	81.6(2)	C8–N1–C3	111.8(4)
N1–Re1–O3	162.4(2)	C8–N1–C4	107.7(4)
C1–Re1–O1	112.1(2)	C2–C1–Re1	118.4(4)
C1–Re1–O2	122.8(2)	C3–C2–C1	110.2(5)
C1–Re1–O3	88.4(2)	C2–C3–N1	108.5(5)
C1–Re1–N1	74.6(2)		

Table 5. Atomic Coordinates of the (γ -Aminoalkyl)rhenium(VII) Oxide **3a**

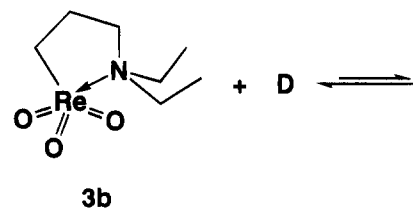
atom	<i>x/a</i>	<i>y/b</i>	<i>z/c</i>
Re1	0.10562(2)	0.080638(2)	0.23030(2)
O1	0.1158(5)	0.1512(3)	0.3693(4)
O2	0.1082(5)	−0.0666(3)	0.2358(4)
O3	0.2799(4)	0.1172(4)	0.1774(4)
N1	−0.1746(5)	0.0494(3)	0.2412(4)
C1	−0.0320(7)	0.1752(6)	0.0778(6)
C2	−0.2147(8)	0.1811(7)	0.0649(7)
C3	−0.2620(7)	0.1544(5)	0.1890(6)
C4	−0.2394(6)	−0.0579(5)	0.1698(6)
C5	−0.4145(7)	−0.0876(7)	0.1821(7)
C6	−0.4301(7)	−0.0977(6)	0.3185(7)
C7	−0.3609(7)	0.0064(6)	0.3906(6)
C8	−0.1863(6)	0.03125(5)	0.3753(5)

structure of the typical example $\text{O}_3\text{ReCH}_2\text{CH}_2\text{CH}_2\text{N}(\text{C}_5\text{H}_{10})$ (**3a**) is shown in Figure 1, selected bond lengths and angles are summarized in Table 4, atomic coordinates are listed in Table 5, and abbreviated crystal data are given in Table 6. The structure resembles that of the known derivative $\text{O}_3\text{ReCH}_2\text{CH}_2\text{CH}_2\text{N}(\text{C}_2\text{H}_5)_2$ (**3b**).⁵ The amino functionality necessarily coordinates in a chelating *cis*-position relative to the alkyl chain termination. The same geometry is found in the solid state *cis*-modification **D** of the aniline adduct of **1**.^{12b} For all other known adducts of organorhenium(VII) oxides with monodentate base ligands, only the *trans*-configuration has been observed. **3a** has a strongly distorted trigonal-bipyramidal structure, with O3 and N1 in the *axial* positions. Nevertheless, the bond distances and angles of the ReO_3 fragment agree pretty well with a tetrahedral geometry. Remarkable is the small angle C1,-

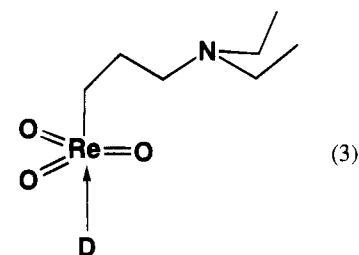
Re1,N1 of 74.6(2)°, suggesting a tetrahedral $\text{O}_3\text{Re}-\text{X}$ core structure in which the atoms C1 and N1 share the remaining tetrahedral corner (X) at the ReO_3 fragment. Only the angle O1,Re,O2 (116.5(2)°) is slightly enlarged due to the steric demand of the piperidyl system. The Re–O bond distances do not indicate any significant *trans*-influence resulting from the amino group. The *envelope* conformation of the five-membered ring implies chirality. The crystal consists of both enantiomers as proven by the space group. The piperidyl ring adopts a chair conformation.



(2) **Structure in Solution.** The labeled derivative **3b**-[¹⁷O] was synthesized to learn more about the geometry in solution. One single ¹⁷O NMR signal is recorded in thf solution at room temperature and above. Broadening of this signal occurs at *ca.* −30 °C (Table 7), and *two* signals standing close together are seen at −60 °C. It is tempting to assume that the solid state structure (see above) is frozen in solution in the slow-exchange domain of the NMR experiment. Fluctuation at higher temperature is likely to involve ring opening of the chelate structure (eq 3, D = thf). Addition of excess quinuclidine leads to a



D = THF, quinuclidine



color change from nearly colorless to yellow with a concomitant shift from $\delta \approx 779$ to 807 ppm (Table 7a). The signal broadens significantly upon cooling to −80 °C. This behavior is once again explained in terms of an equilibrium (eq 3, D = quinuclidine): quinuclidine is a much stronger donor than thf, so even at −80 °C the ligand exchange continues. Attempts to isolate this adduct resulted in a mixture of quinuclidine and **3b**, indicating reverse dissociation.

An oxygen exchange is seen when a thf solution of **3b** is treated with **1**-[¹⁷O]. This exchange is somewhat slower than the oxo exchange between **1** and OsO_4 . **3a** shows a similar behavior.

The oxyfunctionalized alkylrhenium(VII) oxide $\text{O}_3\text{ReCH}_2\text{CH}_2\text{CH}(\text{CH}_3)\text{OCH}_3$ (**4**) was synthesized for the sake of comparison. This complex also shows a fluxional geometry in solution. Cooling to −80 °C in thf leads to a rigid geometry, comparable to the situation of **3a,b** at −60 °C. Addition of

Table 6. Abbreviated Crystal Data for $\text{O}_3\text{ReCH}_2\text{CH}_2\text{CH}_2\text{N}(\text{C}_5\text{H}_{10})$ (**3a**)

formula	$\text{C}_8\text{H}_{16}\text{NO}_3\text{Re}$
M_r	360.43
crystal system	monoclinic
a (pm)	832.7(2)
b (pm)	1151.6(1)
c (pm)	1086.4(2)
β (deg)	101.54(7)
V (10^6 pm^3)	1020.7(3)
space group	$P2_1/c$
D_{calc} (g cm^{-3})	2.35
Mo $K\alpha$ (pm)	71.073
Z	4
$F(000)$	680
μ (cm^{-1})	120.4
θ range (deg)	$1 < \theta < 25$
scan mode	ω scan
temp ($^\circ\text{C}$)	-50 ± 3
no. of reflns measd	3593
no. of reflns with negative intensity	218
no. of unique reflns	1747
no. of reflns used for refinement, $I/\sigma(I) > 0.0$	1747
no. of refined parameters	183
parameters of Tukey and Prince ¹² weighting scheme	$p1 = 0.611, p2 = -0.294, p3 = 0.0399, p4 = 0.112$
max, min electron density in ΔF map ($\text{e } \text{\AA}^{-3}$)	+0.95, -1.48
R^a	0.028
R_w	0.017

$$^a R = \sum(|F_o| - |F_c|)/\sum|F_o|. \quad R_w = [\sum w(|F_o| - |F_c|)^2/\sum w F_o^2]^{1/2}.$$

Table 7(a) ^{17}O NMR Data for **3b** and Its Quinuclidine Adduct in thf

cpd	$\delta(^{17}\text{O})$ (ppm)	$\Delta\nu_{1/2}$ (Hz)	temp ($^\circ\text{C}$)
3b	779	80	20
3b	777	210	-30
3b	777	170	-60
	769	130	
3b	775	200	-80
	767	170	
3b + quinuclidine	807	80	20
3b + quinuclidine	814	340	-30
3b + quinuclidine	817	1400	-80

(b) ^{17}O NMR Data for **4** and Its Quinuclidine Adduct in thf

cpd	$\delta(^{17}\text{O})$ (ppm)	$\Delta\nu_{1/2}$ (Hz)	temp ($^\circ\text{C}$)
4	807	130	20
4	802	380	-30
4	798	380	-80
	759	450	
4 + quinuclidine	911	170	20
4 + quinuclidine	915	360	-30

quinuclidine causes a much stronger low-field shift as compared to the case of the latter complexes (Table 7b), indicating that ether-type oxygen ligands are weaker donors at heptavalent rhenium than nitrogen ligands. The strong Lewis base quinuclidine forms an adduct with **4**; the strong low-field shift ($\delta(^{17}\text{O}) = 911$ ppm) compares well with the quinuclidine adducts of **1** ($\delta(^{17}\text{O}) = 923$ ppm) and **2** ($\delta(^{17}\text{O}) = 920$ ppm).

Conclusion

Lewis-base adducts of organorhenium(VII) oxides undergo exchange phenomena in solution. Exchange of both the base ligands and the oxo ligands occurs at room temperature. Rigid geometries are observed at lower temperatures. Donor solvents facilitate the exchange of the Lewis base ligands. When $\text{R-ReO}_3\cdot n\text{L}$ ($n = 1, 2$) are used as selective olefin epoxidation catalysts, moderate to strong Lewis bases L and weak (or non-) donating solvents should therefore be applied. It is not necessary to synthesize the $\text{R-ReO}_3\cdot n\text{L}$ compounds before use. Because of the equilibria occurring in solution adding a (moder-

ate) excess of the ligand L to a solution of R-ReO_3 should have the same effect. N- and O-functionalized alkylrhenium-(VII) oxides show a fluxional geometry at higher temperatures. N-Donor functions exhibit a much stronger coordination of heptavalent rhenium than O-donors. Addition of strong nitrogen Lewis bases to N- and O-functionalized complexes effects cleavage of the intramolecular donor adducts, thus yielding (intermolecular) Lewis-base adducts.

Experimental Section

All reactions were performed with standard Schlenk techniques in oxygen-free and water-free nitrogen atmosphere. Solvents were dried with standard methods and distilled under N_2 . Infrared spectra were recorded on a Perkin-Elmer 1600 series FTIR spectrometer (resolution 4 cm^{-1}); the ^1H and ^{17}O NMR spectra, at 399.78 and 54.21 MHz, respectively, on a FT-JEOL GX 400 instrument. All NMR solvents were "freeze-pump-thaw" degassed and stored over molecular sieves before use. All compounds used for exchange experiments were studied separately for comparison. Elemental analyses were performed in the microanalytical laboratory of our institute. Mass spectra were obtained with Finnigan MAT 311A and MAT 90 spectrometers. Re_2O_7 (Degussa), quinuclidine (Aldrich), and aniline (Aldrich) were used as received. ^{17}O -enriched **3** and **4** were prepared from ^{17}O -enriched Re_2O_7 (dme) according to refs 13 and 17. For the preparation of ^{17}O -labeled Re_2O_7 and **1**, see ref 13. Bis[3-(*N*-piperidyl)-*n*-propyl]zinc was prepared as described for bis[3-(*N,N*-diethylamino)-*n*-propyl]zinc¹⁸ (**2**). Base adducts of **3** and **4** were prepared according to refs 3e and 12c.

(1) **General Procedure for the Preparation of Base Adducts 1a-c of Methyltrioxorhenium.** A 0.5 g (2.0 mmol) quantity of **1** is dissolved in 5–10 mL of Et_2O , and 2 mmol of N-base is added (either as a solid or dissolved in 5 mL of *n*-pentane or Et_2O ; room temperature). The solution immediately turns yellow, and a yellow precipitate forms. The mixture is stirred for 30 min and then concentrated to 2 mL. The

- (17) (a) Kiprof, P.; Herrmann, W. A.; Kühn, F. E.; Kleine, M.; Elison, M.; Scherer, W.; Rypdal, K.; Volden, H. V.; Gundersen, S.; Haaland, A. *Bull. Soc. Chim. Fr.* **1992**, 129, 655–662. (b) Herrmann, W. A.; Roesky, P. W.; Kühn, F. E.; Elison, M.; Artus, G.; Scherer, W.; Romão, C. C.; Lopes, A.; Bassett, J. M. *Inorg. Chem.*, submitted for publication.
- (18) (a) Thiele, K. H.; Langguth, E.; Müller, G. E. *Z. Anorg. Allg. Chem.* **1980**, 462, 152–158. (b) Thiele, K. H.; Heinrich, M.; Brüser, W.; Schröder, S. *Z. Anorg. Allg. Chem.* **1977**, 432, 221–230.

solution is cooled to 0 °C, and the mother liquor is filtered off. The remaining residue is washed with 5 mL of *n*-pentane and dried in an oil pump vacuum. Yields: 80–100%. Spectroscopic data and elemental analyses are identical with the data of ref 12.

(2) Preparation of [3-(*N*-piperidyl)-*n*-propyl]trioxorhenium(VII) (3a). A solution of 0.50 g (1.5 mmol) of bis[3-(*N,N*-diethylamino)-*n*-propyl]zinc in 5 mL of thf is dropwise added at –78 °C to a solution of Re₂O₇ (1.5 g, 3 mmol) in 30 mL of thf. The mixture is stirred for 1 h at –78 °C and then warmed to 0 °C. To precipitate the formed zinc perchlorate, the mixture is cooled to –20 °C for 1 h. After filtration, the blue-violet solution is concentrated to 5 mL and then cooled to –30 °C. Analytically pure **3a** is isolated as blue crystals after several days.

Air-stable single crystals were obtained by crystallization from thf. Anal. Calcd for C₈H₁₆NO₃Re: C, 26.66; H, 4.47; N, 3.89; Re, 51.66. Found: C, 27.00; H, 4.58; N, 3.83; Re, 51.04. IR [KBr, cm⁻¹]: ν(Re=O) 920.2 (vs), 959.8 (vs), 977.0 (m). ¹H NMR [thf-*d*₆, 400 MHz, 20 °C, ppm]: δ(C⁶-H₂) 1.58 [quin, 2H, ³J = 6.1 Hz]; δ(C⁵-H₂) 1.69 [quin, 4H, ³J = 6.1 Hz]; δ(C⁴-CH₂) 2.50 [tr, 4H, ³J = 6.1 Hz]; δ(C³-H₂) 2.83 [tr, 2H, ³J = 6.4 Hz]; δ(C²-H₂) 2.94 [m, 2H]; δ(C¹-H₂) 3.42 [tr, 2H, ³J = 7.3 Hz]. Mass spectra, electron impact at 70 eV, *m/z*, ¹⁸⁷Re, correct isotope pattern: 361 [M⁺]; 126 [M – ReO₃⁺]; 98 [N-piperidyl – CH₂⁺].

(3) Preparation of (3-Methoxy-*n*-butyl)trioxorhenium(VII) (4). This compound was prepared as described for **3a**. Analytically pure **4** can be isolated as yellow crystals. Yield: 0.490 g (75%). Anal. Calcd for C₅H₁₁O₄Re: C, 18.69; H, 3.45; O, 19.92; Found: C, 18.92; H, 3.43; O, 20.29. IR [KBr, cm⁻¹]: ν(Re=O) 940.3 (vs), 972.4 (vs). ¹H NMR [thf-*d*₆, 400 MHz, 20 °C, ppm]: δ(C⁴-H₃) 1.18 [d, 3H, ³J = 6.1]; δ(C²-H) 2.24 [m, 1H]; δ(C²-H) 2.94 [m, 1H]; δ(C¹-H₂) 3.37 [m, 2H]; δ(C³-H) 3.49 [m, 1H]; δ(C⁵-H₃) 3.51 [s, 3H]. ¹³C NMR [thf-*d*₆, 100.54 MHz, 20 °C, ppm]: δ(C⁴) 17.4; δ(C²) 39.0; δ(C¹) 39.2; δ(C⁵) 56.8; δ(C³) 79.2.

(4) Crystal Structure Determination of the (γ-Aminoalkyl)-rhenium(VII) Oxide 3a. Crystals were obtained from a thf solution at –30 °C. A deep blue crystal fragment was mounted in a Lindeman capillary on an Enraf-Nonius CAD4 diffractometer with κ geometry. Empirical absorption corrections were applied to the data set.¹⁹ The structure was solved by the Patterson method (SHELXS-86),²⁰ and refinements were carried out using the program CRYSTALS.²¹ All atoms could be found by difference Fourier techniques. Hydrogen atoms were refined with isotropic temperature factors. For details see Table 6.

Acknowledgment. This work was supported by the Herrmann Schlosser Foundation through a graduate fellowship to F.E.K. We are indebted to DEGUSSA AG (Prof. Offermanns and Dr. Gerhartz) for a generous gift of Re₂O₇ and the Stiftung Volkswagenwerk for financial support. We also thank the DAAD and the European Community for a grant to J.D.G.C.

Supplementary Material Available: Tables of hydrogen atom parameters, complete bond distances and bond angles, and anisotropic displacement parameters for **3a** and figures showing selected variable-temperature ¹⁷O NMR spectra of compounds described in the text (10 pages). Ordering information is given on any current masthead page.

IC941229G

-
- (19) Frenz, B. A. *ENRAF-NONIUS SDP-plus Structure Determination Package*, Version 4.0; Enraf-Nonius: Delft, The Netherlands, 1988.
 (20) Sheldrick, G. M. SHELXS-86. Universität Göttingen, Germany, 1986.
 (21) Watkin, D. J.; Betteridge, P. W.; Carruthers, J. R. *CRYSTALS User Manual*; Oxford University Computing Laboratory: Oxford, England, 1986.
 (22) Spek, A. L. PLATON-93: An Integrated Tool for the Analysis of the Results of a Single Crystal Structure Determination *Acta Crystallogr.* **1990**, *A46/C34*.